# Statistics of flame topology in turbulent spray flame water droplet interaction

R. Concetti[1], J. Hasslberger[1], N. Chakraborty[2] and M. Klein[1]
[1]Institute of Applied Mathematics and Scientific Computing, Bundeswehr University Munich, Neubiberg, Germany
[2]School of Engineering, Newcastle University, Newcastle Upon Tyne, United Kingdom

## 1 Introduction

Due to the increasingly stringent rules on internal combustion engine emissions, especially related to $NO_x$, new technical solutions are urgently needed. One attractive possibility is to inject liquid water into the combustion chamber which reduces the flame temperature via the heat sink associated to evaporating droplets [1]. It is worth noting that water stands out by a very high liquid-gas density ratio as well as the highest specific heat and latent heat of vaporization of all liquids. The water injection technology has already demonstrated its potential to increase the performance of automotive and aircraft propulsion. Furthermore, the water droplet flame interaction is relevant to fire suppression and explosion mitigation. This study focuses on the flame topology response of turbulent spray flames due to water droplet interaction. As it has been demonstrated by Dopazo et al. [2], the combined measurements of Gauss and mean curvature of scalar isosurfaces allow for the classification of flame topologies with respect to concave/convex ellipsoid, cylinder and saddle structures of the wrinkled (flame) surface. Characterizing the structure of the flame, reaction progress variable and normalized temperature are considered here as the relevant scalar isosurfaces. Subjected to a constant water droplet stream from the inlet, statistically planar turbulent n-heptane/air spray flames (i.e. partially premixed) are investigated for this purpose by means of carrier-phase direct numerical simulation (DNS).

## 2 Computational method

Based on a high order finite difference discretization for the gas phase Eulerian representation and a Lagrangian point particle representation for both n-heptane fuel droplets and water droplets, a two-way coupled hybrid scheme has been implemented in SENGA+, a three-dimensional compressible DNS code [3]. Similar to several earlier DNS studies (e.g. [5]) on n-heptane spray flames without water addition, the gas-phase chemical reaction is described by a one-step irreversible Arrhenius-type ansatz [4] for the purpose of computational economy. Imposing periodic boundaries in both lateral directions, a canonical inflow-outflow configuration has been realized within a rectangular domain of size $30\delta_{st} \times 20\delta_{st} \times 20\delta_{st}$, where $\delta_{st}$

Correspondence to: riccardo.concetti@unibw.de 

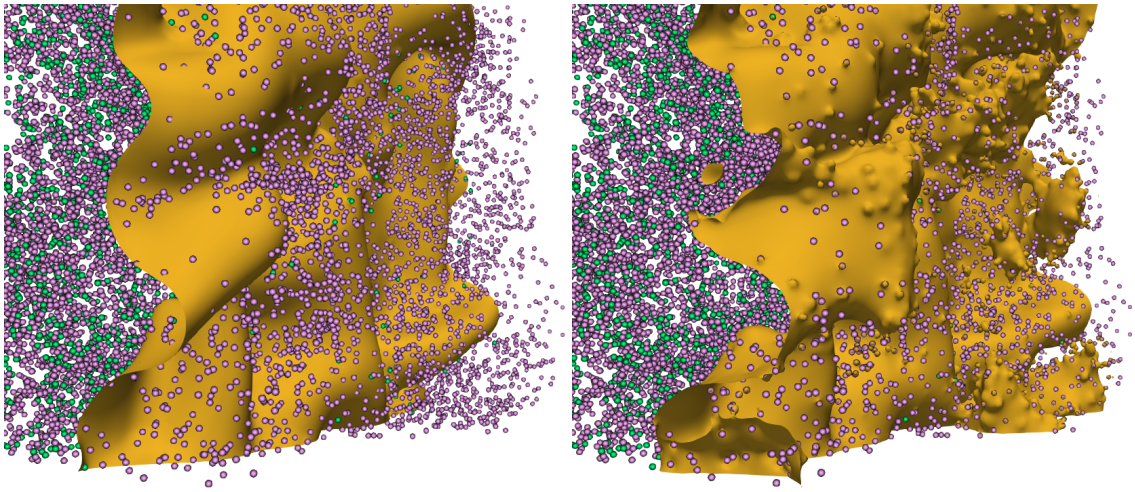

Figure 1: Isosurfaces of reaction progress variable $c = 0.85$ on the left and normalized temperature $T = 0.85$ on the right at $t/t_{chem} = 1.1$ for the spray flame case with water addition. Not-to-the-scale spheres indicate the fuel droplets (green) and water droplets (pink).

is the thermal flame thickness of the laminar stoichiometric premixed flame without water addition. Spatial discretization by $384 \times 256 \times 256$ grid points ensures to resolve the thermal flame thickness as well as the Kolmogorov length scale. Generated by a pseudo-spectral method, the turbulent flow field following a Batchelor-Townsend energy spectrum is initially imposed throughout the domain and continuously maintained at the inlet. A turbulence intensity of $u'/S_L = 4$ and an integral turbulent length scale of $L_{11}/\delta_{st} = 2.5$ are investigated here, where $S_L$ is the burning velocity of the unstretched laminar stoichiometric premixed flame without water addition. Considering the fuel in liquid and gaseous phases, an overall equivalence ratio $\phi_{ov} = \phi_l + \phi_g$ of unity is maintained throughout the simulation. The overall water loading $Y_W = Y_W^l + Y_W^g$ accounts for the water mass fraction in both phases but excludes the product water generated by the chemical reaction. The investigated value of $Y_W = 0.1$ lies in the technically relevant range and is also comparable to earlier experimental studies. Whereas the size of initially mono-disperse fuel droplets is $a_d/\delta_{st} = 0.04$, the size of initially mono-disperse water droplets is varied between $a_d/\delta_{st} = 0.02$ and $0.04$ while keeping all other parameters constant. Strong differences regarding the effect of water addition can be observed for these parameters. The reaction progress variable $c$ can be defined as

$$c = \frac{(Y_O^0 - Y_O)Y_O/s + Y_F Y_O^0 s - Y_F Y_O s}{(Y_O^0 - Y_O)Y_O/s + Y_F Y_O^0 s + Y_F Y_O}, \tag{1}$$

where $Y_F$, $Y_O$ are the fuel and oxidizer mass fraction (superscript 0 refers to unburned conditions) and $s = 3.52$ is the stoichiometric mass ratio of oxidizer to fuel (n-heptane). The complexity of the spray flame water droplet interaction can be inferred from the three-dimensional view in Fig. 1. Isosurfaces of $c$ and normalized temperature $T$ are clearly non-conforming, which is mainly due to the heat sink associated to evaporating water droplets. The localized dimples on the $T = 0.85$ isosurface are a direct consequence of this cooling effect. This behavior is in contrast to unity Lewis number premixed flames, where $c = T$ holds. Also note that the highly volatile fuel droplets (latent heat of vaporization of 315.0 kJ/kg) rarely reach the hot gas side of the flame, whereas the water droplets penetrate far into the post-flame region ($c = 1$) according to their low volatility (latent heat of vaporization of 2258.0 kJ/kg).

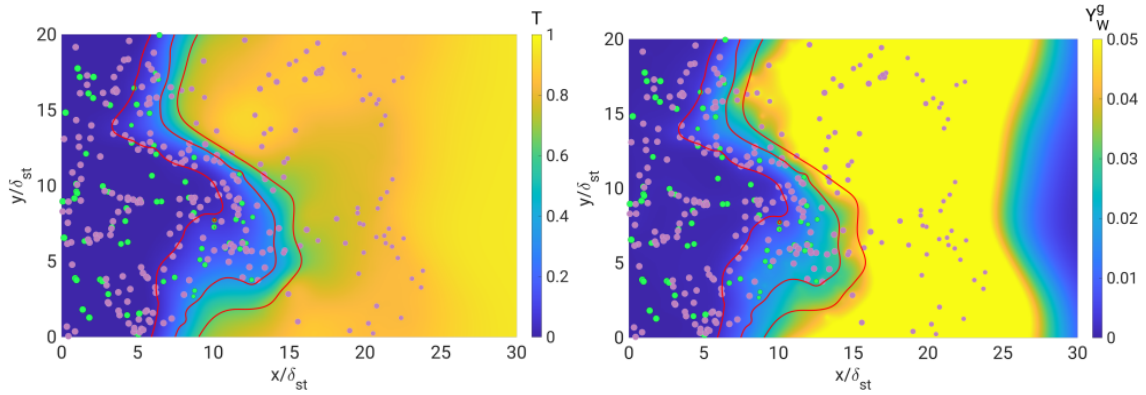


Figure 2: Mid-plane contours of normalized temperature $T$ (left) and steam mass fraction $Y_W^g$ exclusive of the product water (right) at $t/t_{chem} = 4.1$. Not-to-the-scale dots indicate the fuel droplets (green) and water droplets (pink), both of initial size $a_d/\delta_{st} = 0.04$. Red isolines represent $c = 0.1, 0.5, 0.9$, respectively.

Table 1: Surface topologies depending on the sign of $k_m$ and $k_g$.

| | $k_m > 0$ | $k_m = 0$ | $k_m < 0$ |
|---|---|---|---|
| $k_g > 0$ | Convex ellipsoid | Non-physical | Concave ellipsoid |
| $k_g = 0$ | Convex cylinder | Plane | Concave cylinder |
| $k_g < 0$ | Convex saddle | Saddle | Concave saddle |

## 3 Results and discussion

The inner structure of the spray flame (enclosed by the red isolines representing $c = 0.1, 0.5, 0.9$, respectively) with water addition is shown in Fig. 2 by means of two-dimensional slices of $T$ and $Y_W^g$ through the domain. The temperature reduction effect due to water droplets can be seen especially in the burned gas region, considering that $T = 1$ corresponds to the adiabatic flame temperature of the stoichiometric premixed flame without water addition. Compared to purely premixed combustion, the temperature is additionally lowered in the spray flame case because the partially premixed combustion takes place under fuel-lean conditions. The steam mass fraction $Y_W^g$, exclusive of the product water, in the flame region remains much smaller than the overall water loading $Y_W = 0.1$. Hence, the dilution effect on reaction zone characteristics is generally small while large steam mass fractions are observed in the post-flame region.

To conduct the curvature analysis of scalar isosurfaces, it is first of all necessary to define the unit normal of the isosurface, that is, $\vec{n}_c = -\nabla c/|\nabla c|$ and $\vec{n}_T = -\nabla T/|\nabla T|$, respectively. Hence, the normal points towards the reactants, or cold gas, when the temperature is considered. The curvature tensor can then be defined as the gradient of the normal vector and the two non-zero eigenvalues are the principal curvatures $k_1$ and $k_2$ of the isosurface at a particular point. The non-zero eigenvalues are always $\leq 2$ in number due to the fact that the derivative of the normal along the normal direction is identical to zero. In other words, $\vec{n}$ is an eigenvector of the curvature tensor and $k_1, k_2$ are the maximum/minimum value of curvature, which occur in perpendicular directions. The mean and Gauss curvature are given by $k_m = (k_1 + k_2)/2$ and $k_g = k_1 k_2$, respectively, and these allow to distinguish different surface topologies according to Table 1. It can be shown that the region with $k_g > k_m^2$ is non-physical (complex curvature region) [2].

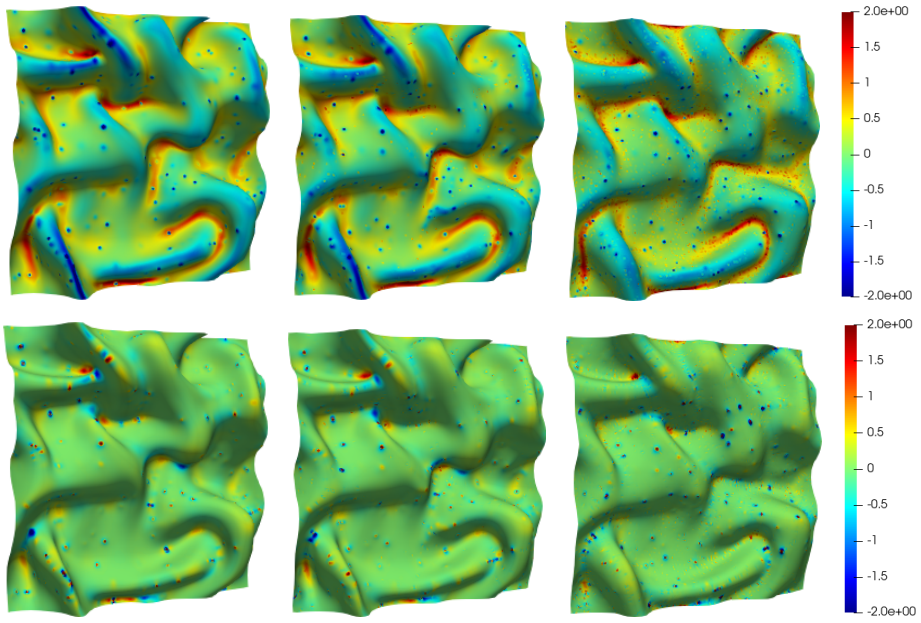


Figure 3: Isosurfaces of $c = 0.5$ at $t/t_{chem} = 1.1$ colored by mean curvature $k_m \times \delta_{st}$ (top row) and Gauss curvature $k_g \times \delta_{st}^2$ (bottom row) for the cases without water droplets (left), water droplets of size $a_d/\delta_{st} = 0.04$ (center) and $a_d/\delta_{st} = 0.02$ (right).

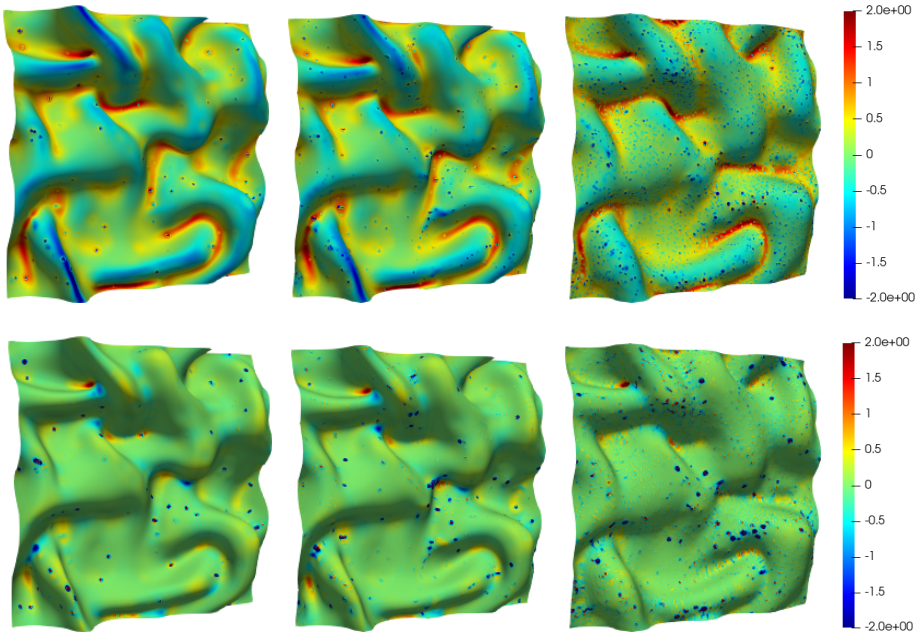


Figure 4: Isosurfaces of $T = 0.5$ at $t/t_{chem} = 1.1$ colored by mean curvature $k_m \times \delta_{st}$ (top row) and Gauss curvature $k_g \times \delta_{st}^2$ (bottom row) for the cases without water droplets (left), water droplets of size $a_d/\delta_{st} = 0.04$ (center) and $a_d/\delta_{st} = 0.02$ (right).

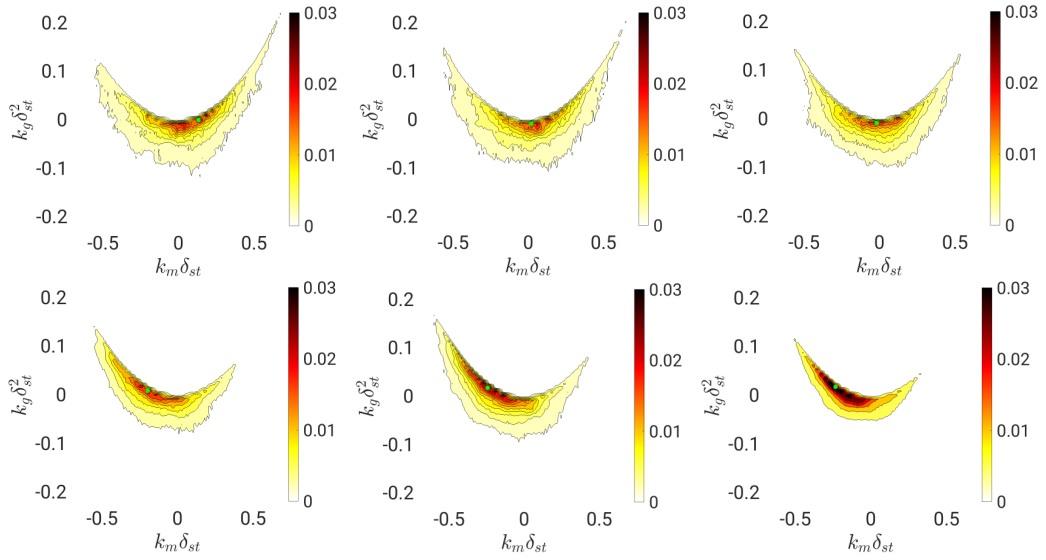


Figure 5: Joint PDF of $k_m \times \delta_{st}$ and $k_g \times \delta_{st}^2$ based on $c$ at $t/t_{chem} = 1.1$ in the regions $0.4 < c < 0.6$ (top row) and $0.7 < c < 0.95$ (bottom row) for the cases without water droplets (left), water droplets of size $a_d/\delta_{st} = 0.04$ (center) and $a_d/\delta_{st} = 0.02$ (right).

Visualizing the Gauss and mean curvature on isosurfaces of $c = 0.5$ and $T = 0.5$, respectively, Figs. 3 and 4 demonstrate the different flame topology response due to fuel and water droplet interaction. The corresponding joint probability density functions (PDF) of $k_m \times \delta_{st}$ and $k_g \times \delta_{st}^2$ are presented in Figs. 5 and 6, respectively. In the region $0.4 < c < 0.6$, reaction progress isosurfaces are characterized by a more symmetric curvature joint PDF with water droplet interaction, hence overcoming the dominance of convex topologies for the spray flame without water injection. In the region $0.7 < c < 0.95$, water droplet interaction yields a narrower curvature joint PDF, indicating flattening of progress variable isosurfaces. The effects become increasingly evident for decreasing water droplet size $a_d/\delta_{st}$ due to faster evaporation (cf. "diameter squared"-law). Normalized temperature isosurfaces are showing the strongest response on the hot gas side of the flame ($0.7 < T < 0.95$), where the water droplet interaction leads to a shift from concave-dominated topologies to a symmetric distribution, mostly representing comparably flat saddle topologies. Regarding the implications of the findings, it is worth mentioning that the surface topology and curvature distribution have important effects on the flame displacement speed and on the evolution of the surface density function (SDF), i.e. $|\nabla c|$. Both these quantities are of pivotal importance to well-established combustion modeling concepts. For example, the relations between the mean curvature and the terms that appear in the SDF transport equation have been analyzed in detail by Chakraborty & Cant [6].

## 4 Concluding remarks

The impact of water droplet addition on statistically planar turbulent spray flames has been studied by means of a novel Euler-Lagrange-Lagrange scheme. It has been found by combined measurements of Gauss and mean curvature that the surface topology of reaction progress isosurfaces is dominated by the highly volatile fuel droplets whereas the effect of low-volatility water droplets is rather reflected by the normalized temperature isosurfaces. However, due to the turbulence dampening effect of evaporating droplets [1], water

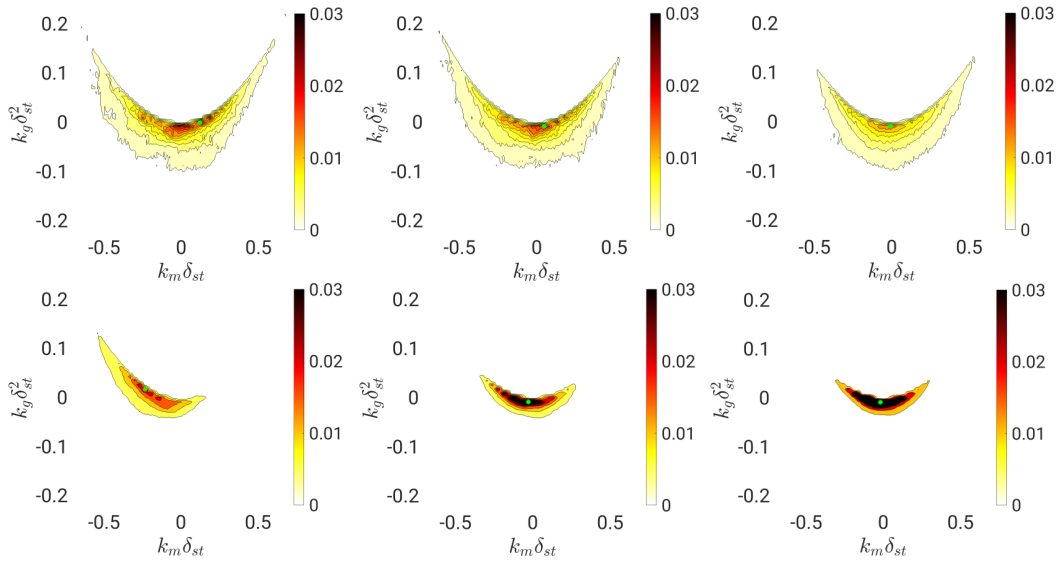


Figure 6: Joint PDF of $k_m \times \delta_{st}$ and $k_g \times \delta_{st}^2$ based on $T$ at $t/t_{chem} = 1.1$ in the regions $0.4 < T < 0.6$ (top row) and $0.7 < T < 0.95$ (bottom row) for the cases without water droplets (left), water droplets of size $a_d/\delta_{st} = 0.04$ (center) and $a_d/\delta_{st} = 0.02$ (right).

injection influences the curvature distribution (and thus flame speed via stretch effects) in additional non-trivial ways.

## References

[1] Hasslberger, J., Ozel-Erol, G., Chakraborty, N., Klein, M., & Cant, S. (2021). Physical effects of water droplets interacting with turbulent premixed flames: A Direct Numerical Simulation analysis. Combustion and Flame, 229, 111404.

[2] Dopazo, C., Martin, J., Hierro, J. (2007). Local geometry of isoscalar surfaces. Physical Review E, 76(5), 056316.

[3] Jenkins, K. W., & Cant, S. (2002). Curvature effects on flame kernels in a turbulent environment. Proceedings of the Combustion Institute, 29(2), 2023-2029.

[4] Fernandez-Tarrazo, E., Sanchez, A. L., Linan, A., & Williams, F. A. (2006). A simple one-step chemistry model for partially premixed hydrocarbon combustion. Combustion and Flame, 147(1-2), 32-38.

[5] Ozel Erol, G., Hasslberger, J., Klein, M., & Chakraborty, N. (2018). A direct numerical simulation analysis of spherically expanding turbulent flames in fuel droplet-mists for an overall equivalence ratio of unity. Physics of Fluids, 30(8), 086104.

[6] Chakraborty, N., Cant, S. (2005). Effects of strain rate and curvature on surface density function transport in turbulent premixed flames in the thin reaction zones regime. Physics of Fluids, 17(6), 065108.